Ultrasound in Med. & Biol., Vol. 00, No. 00, pp. 1–9, 2022

0301-5629/$ - see front matter

https://doi.org/10.1016/j.ultrasmedbio.2022.04.219

● *Original Contribution*

# EVALUATION OF TISSUE STIFFNESS AROUND LESIONS BY SOUND TOUCH SHEAR WAVE ELASTOGRAPHY IN BREAST MALIGNANCY DIAGNOSIS

Ya-Yun Cui,*,† Nian-An He,† Xian-Jun Ye,† Lei Hu,† Li Xie,† Wen Zhong,‡ and Chao-Xue Zhang*

* Department of Ultrasound, First Affiliated Hospital of Anhui Medical University, Hefei, Anhui, China; † Department of Ultrasound, First Affiliated Hospital of USTC, Division of Life Sciences and Medicine, University of Science and Technology of China, Hefei, Anhui, China; and ‡ Department of Pathology, First Affiliated Hospital of USTC, Division of Life Sciences and Medicine, University of Science and Technology of China, Hefei, Anhui, China

(*Received* 16 *January* 2022; *revised* 9 *March* 2022; *in final form* 29 *April* 2022)

**Abstract—The aim of the study described here was to assess the evaluation of tissue stiffness around lesions by sound touch shear wave elastography (STE) in breast malignancy diagnosis. This was an institutional ethics committee–approved, single-center study. A total of 90 women with breast masses examined with conventional ultrasound and STE were eligible for enrollment from December 2020 to July 2021. The maximum and mean elastic values of masses, $E_{max}$ and $E_{mean}$, were determined. Shell function was used to measure the maximum and mean elastic values of tissues around masses in annular shells 0.5, 1.0, 1.5 and 2.0 mm wide, recorded as corresponding $E_{max\text{-}shell}$ and $E_{mean\text{-}shell}$. All parameters were analyzed and compared with histopathologic results. Receiver operating characteristic curves were constructed to assess diagnostic performance. Logistic regression analysis was conducted to determine the best diagnostic model. Collagen fiber content of tissues around breast lesions was evaluated using Masson staining and ImageJ software. Ninety women with breast masses were included in this study; 50 had benign (mean diameter 15.84 ± 4.39 mm) and 40 had malignant (mean diameter 17.40 ± 5.42 mm) masses. The diagnostic value of $E_{max\text{-}shell\text{-}2.0}$ was the highest (area under the curve = 0.930) with a sensitivity of 87.5% and specificity of 88%. According to stepwise logistic regression analysis, $E_{max\text{-}shell\text{-}2.0}$ and age were independent predictors of malignancy. $E_{max\text{-}shell\text{-}2.0}$ was also found to be highly correlated with the collagen fiber content of tissue in the malignant group ($r$ = 0.877). Tissue stiffness around lesions measured by STE is a useful metric in identifying malignant breast masses by reflecting collagen fiber content, and $E_{max\text{-}shell\text{-}2.0}$ performs best.**
**(E-mail: zcxay@163.com)**


*Key Words:* **Breast, Sound touch elastography, Shear wave elastography, Ultrasound.**

## INTRODUCTION

Currently, mammography, ultrasound and magnetic resonance imaging (MRI) are commonly used to evaluate breast lesions. Screening mammography reduces mortality from breast cancer through early detection; however, the sensitivity of mammography decreases in dense breasts, while the risk of breast cancer increases with breast density (Peairs et al. 2017; Geisel et al. 2018; Mitchell 2021). Additionally, the ionizing radiation damage cannot be ignored (Rossi et al. 2019). MRI, which is relatively expensive, time-consuming and not suitable for all patients, plays a complementary imaging role to mammography. Ultrasound has become an indispensable tool in breast imaging today, particularly in women with dense breast tissue. It has good sensitivity in detecting breast masses and is well tolerated without ionizing radiation (Winters et al. 2017). Nevertheless, it should be noted that conventional ultrasound has low specificity in diagnosing breast lesions (Berg et al. 2015). Therefore, it is necessary to find better methods to improve the accuracy of differentiating malignant masses from benign masses.

Ultrasound elastography, based either on strain or on shear waves, is an ultrasound technique able to assess tissue stiffness by providing information on its elasticity (Mesurolle et al. 2019). As malignant masses tend to be stiffer than benign masses, we can use elastic ultrasound to diagnose malignant masses (Ophir et al. 1991; Barr et al. 2015). Research has revealed that malignant lesions have an abundance of collagen fibers and the fibrous tissue structures affect tissue stiffness

Address correspondence to: Chao-Xue Zhang, Department of Ultrasound, First Affiliated Hospital of Anhui Medical University, No. 218 Jixi Road, Shushan District, Hefei, Anhui, 230022, China. E-mail: zcxay@163.com

(Shi et al. 2018; Choi et al. 2019). Several studies have determined that using elastography ultrasound to measure the internal elasticity of masses is valuable in differentiating benign and malignant breast lesions (Balleyguier et al. 2013; Barr et al. 2015; Ricci et al. 2017; Farooq et al. 2019; Altıntas et al. 2021). Considering that the internal components of breast lesions are usually heterogeneous because of cystic changes, hemorrhage and calcification, which may influence elasticity values, more and more attention has been paid to the stiffness of the tissue around breast masses in recent years (Zhou et al. 2014a, 2014b; Xiao et al. 2016; Zhang et al. 2019).

Sound touch shear wave elastography (STE) is a novel real-time shear wave elastographic technology available on the Resona 7 diagnostic ultrasound system (Mindray Medical International, Shenzhen, China). It has been widely used to measure the stiffness of liver, thyroid, breast and other tissues (Zhang et al. 2018; Xia et al. 2019). The shell measurement function of STE enables quantitative assessment of peripheral tissues stiffness. Several studies have indicated that STE had the potential to diagnose breast malignancy through the quantitative evaluation of tissue stiffness around lesions (Dong et al. 2019). However, there is no consensus as to which area around breast lesions should be measured to predict malignant breast lesions.

This study used the STE technique to measure elasticity values in different areas around breast masses and investigated their value in the diagnosis of malignant breast masses. Additionally, the correlation between the collagen fiber content of tissues around a lesion and its elasticity value was also analyzed to further explore the mechanism underlying peripheral tissue elasticity in identifying malignancy.

## METHODS

### *Patients*

From December 2020 to July 2021, 133 consecutive patients with breast masses that were palpable or detected by mammography/ultrasound were registered in this study for conventional ultrasound and STE examinations. The inclusion criteria were as follows: (i) breast mass size between 5 and 30 mm; (ii) solid or nearly solid breast mass (cystic composition <20%); (iii) no treatment, such as breast surgery, radiotherapy or chemotherapy, before enrollment. Exclusion criteria were (i) masses with Breast Imaging Reporting and Data System (BI-RADS) scores <3 based on conventional ultrasound; (ii) lack of normal breast tissues surrounding masses (<3 mm in thickness); (iii) non-standard elastographic images; (iv) no final histological results. Finally, 90 women with breast masses were included in this study. Figure 1 is a flowchart illustrating the patient selection

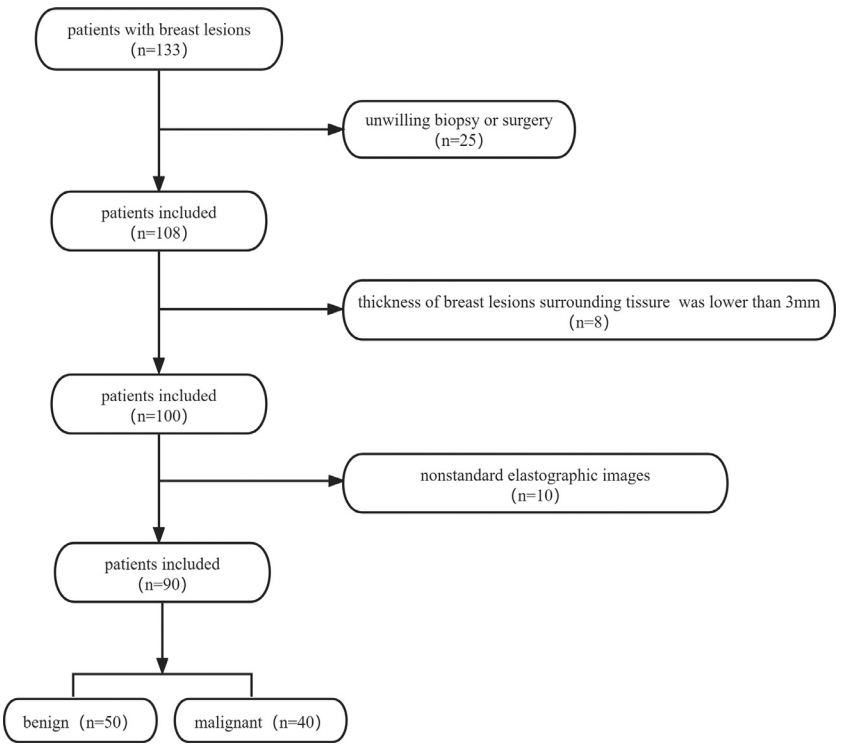


Fig. 1. Flowchart illustrating patient selection process.

process. This retrospective study complied with the Declaration of Helsinki and was approved by the institutional ethics committee of the First Affiliated Hospital of USTC, Division of Life Sciences and Medicine, University of Science and Technology of China. Informed consent to the study was obtained from all participants.

*Ultrasound equipment*

For conventional ultrasound and STE examinations, the L11-3U (bandwidth frequency = 3−11 MHz) linear array transducer of Resona 7 diagnostic ultrasound system (Mindray Medical International) was employed. The diagnostic system was equipped with a unique shell quantification toolbox, which could measure the elastic modulus values of the tissue (0.5− 9 mm) surrounding breast masses in 0.5-mm increments.

*Image acquisition*

Patients needed to maintain a supine position with the breast and axilla fully exposed. Continuous multi-angle and multi-section exploration was conducted in the breast by a radiologist with 15 y of experience in breast ultrasound. In patients found to have multiple masses, the most suspicious one was selected for grading according to the terminology of the BI-RADS lexicon (Lin et al. 2018). And when multiple lesions were in the same BI-RADS category, the lesion with the largest diameter was selected. The maximum diameter of the mass was measured. The distance between the front margin of the mass and the epidermis was recorded. The following STE imaging would be performed by the other doctor with 4 y of experience in STE, who was blinded to BI-RADS results. A standard gray-scale section was first found, and the target lesion was placed in the center of the screen; then STE mode was activated. STE and gray-scale images were simultaneously displayed on the monitor. Next, a rectangular region of interest (ROI) was set to include the entire breast mass and surrounding tissue. It should be noted that obvious cystic parts or calcifications cannot be included. The transducer was positioned perpendicularly and as gently as possible. Participants were required to hold their breath on acquisition of the elastic image. These approaches were used to prevent obvious artifacts, which may influence the elastic modulus map. The reliability of the STE images was assessed through the quality control chart (QCC), which appeared at the top right corner of the screen. Once the image was stabilized, the contours of the lesion were traced and delineated manually by the doctor with 4 y of experience in STE using a sliding trackball on the gray-scale image, and the boundary of the mass was simultaneously displayed on the STE mode. Then, the maximum and mean Young's moduli of the mass could be calculated and recorded as $E_{max}$ and $E_{mean}$. Afterward, "shell" function key on the control panel was pressed. By adjusting the "shell" to 0.5, 1.0, 1.5 and 2.0 mm, the ultrasound system automatically calculated the maximum elastic modulus and mean elastic modulus of the "shell" area, which were recorded as $E_{max\text{-}shell\text{-}0.5}$, $E_{mean\text{-}shell\text{-}0.5}$, $E_{max\text{-}shell\text{-}1.0}$, $E_{mean\text{-}shell\text{-}1.0}$, $E_{max\text{-}shell\text{-}1.5}$, $E_{mean\text{-}shell\text{-}1.5}$, $E_{max\text{-}shell\text{-}2.0}$ and $E_{mean\text{-}shell\text{-}2.0}$. Each elasticity value was measured three times. Finally, average values of the data were calculated and incorporated into the study.

*Histopathological examination*

Histopathological examination was used as the reference standard. Histopathological diagnosis was performed by a pathologist with 15 y of experience. First, collagen fibers of breast masses and surrounding tissues were stained with the Masson staining method. Second, these histopathologic slides were scanned with a Motic digital slice scanning system (version 1.0, Motic Co., Ltd, Xiamen, China), and whole-slide imaging (WSI) was used. The WSI images of all breast masses and peripheral tissues at sizes of 0.5, 1.0, 1.5 and 2.0 mm were extracted with Photoshop (version CS6, Adobe Systems, Inc., San Jose, CA, USA). Then, these images were compared with the pre-operative ultrasound images. Afterward, ImageJ software (version 1.48; National Institutes of Health, Bethesda, MD) was used to calculate collagen fiber content in different regions around masses from the images extracted with Photoshop (Fig. 2A−E).

*Statistical analysis*

Statistical analyses were performed with SPSS version 23.0 software (IBM, Armonk, NY, USA). Continuous data satisfying the normal distribution are expressed as the mean ± standard deviation (SD), and benign and malignant lesions were compared with the independent *t*-test. Otherwise, data on the skewness distribution are described as the median and interquartile, and comparisons between groups were performed with the Mann−Whitney *U*-test. Categorical data are expressed as absolute numbers and percentages. Receiver operating characteristic curve (ROC) analyses were conducted to assess the diagnostic performance of $E_{max}$, $E_{mean}$ and different measurements of $E_{max\text{-}shell}$ and $E_{mean\text{-}shell}$. Sensitivity, specificity and area under the curve (AUC) were also calculated. The best cutoff value was determined with Youden's index. Univariate analysis was performed to identify potential factors predictive of malignancy. After univariate analysis, a binary logistic regression model was used for multivariate analysis while adjusting for any predictive factors found to be associated with malignancy in the univariate analysis ($p < 0.10$). We adopted a stepwise method, and significant factors with

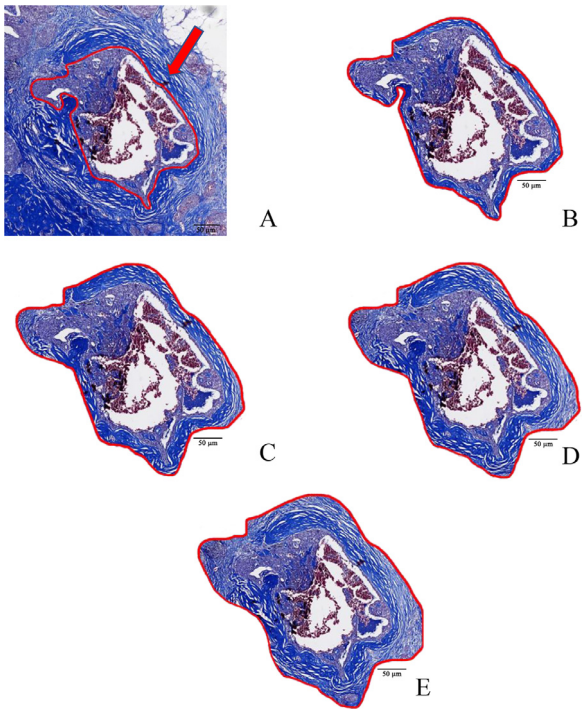


Fig. 2. Masson stain was applied to collagen fibers surrounding breast masses on whole-slide images of the histopathologic slides (A, *red arrow* points to collagen fibers). Images of breast masses and peripheral tissues of 0.5 mm (B), 1 mm (C), 1.5 mm (D) and 2 mm (E) were extracted by Photoshop on whole-slide images of breast masses and histopathologic slides.

$p$ values <0.05 were retained in the final model. The likelihood ratio (LR) test and Hosmer–Lemeshow test were applied to assess the model's goodness of fit. Conventional ultrasound tests considered BI-RADS classes higher than 3 as positive for malignancy; other classes were considered negative. Correlations between different $E_{\text{max-shell}}$ values and the corresponding collagen fiber contents on histopathologic findings were evaluated with the Spearman correlation coefficient and divided into four grades: weak ($r < 0.5$), moderate ($0.5 \leq r < 0.7$), strong ($0.7 \leq r < 0.9$) and very strong ($0.9 \leq r < 1$) (Mukaka 2012). A $p$ value <0.05 was considered to indicate statistical significance.

## RESULTS

*Study population*

Ninety patients with 50 benign masses (55.56%) and 40 malignant masses (44.44%) were finally included in this study. The most common benign pathological pattern was fibroadenoma; invasive ductal carcinoma was the most frequent malignant pattern. Histopathological results of the benign and malignant masses are detailed in Table 1.

Table 1. Histopathological results and BI-RADS category of benign and malignant lesions

| Pathologic finding | n (%) | BI-RADS category | | | | |
|---|---|---|---|---|---|---|
| | | 3 | 4a | 4b | 4c | 5 |
| Benign | 50 (55.56) | 16 | 30 | 4 | 0 | 0 |
| Fibroadenoma | 28 (31.11) | 9 | 17 | 2 | 0 | 0 |
| Intraductal papilloma | 5 (5.56) | 2 | 2 | 1 | 0 | 0 |
| Adenosis | 11 (12.22) | 3 | 8 | 0 | 0 | 0 |
| Inflammation | 3 (3.33) | 1 | 2 | 0 | 0 | 0 |
| Hyperplastic nodule | 2 (2.22) | 0 | 1 | 1 | 0 | 0 |
| Tubular adenoma | 1 (1.11) | 1 | 0 | 0 | 0 | 0 |
| Malignant | 40 (44.44) | 2 | 5 | 10 | 12 | 11 |
| Invasive ductal carcinoma | 29 (32.22) | 2 | 2 | 6 | 10 | 9 |
| Invasive lobular carcinoma | 1 (1.11) | 0 | 0 | 1 | 0 | 0 |
| Ductal carcinoma *in situ* | 9 (10.00) | 0 | 3 | 3 | 1 | 2 |
| Mucinous carcinoma | 1 (1.11) | 0 | 0 | 0 | 1 | 0 |

BI-RADS = Breast Imaging Reporting and Data System.

The mean ages of patients with malignant and benign masses were 53.30 ± 12.24 y (range: 26–89 y) and 39.78 ± 10.23 y (range: 20–59 y), respectively. Statistically significant differences in age were observed between patients with malignant and benign masses ($p < 0.05$). There was no significant difference in maximum diameter between malignant (17.40 ± 5.42 mm) and benign (15.84 ± 4.39 mm) masses ($p > 0.05$). Moreover, the mean distance between the front margin of malignant masses and the epidermis was 7.80 ± 3.53 mm, whereas that for the benign masses was 8.62 ± 3.64 mm, and the difference was of no significance ($p > 0.05$).

*Diagnostic performance of conventional ultrasound*

The AUC of conventional ultrasound was 0.635 (95% confidence interval [CI]: 0.521, 0.749). The sensitivity, specificity, positive prediction value (PPV) and negative prediction value (NPV) were 95.0%, 32.0%, 70.4% and 94.4%, respectively (Table 2).

*Diagnostic performance of STE parameters inside masses ($E_{max}$, $E_{mean}$)*

The $E_{\text{max}}$ and $E_{\text{mean}}$ values of malignant lesions were significantly higher than those of benign lesions ($p < 0.05$) (Figs. 3 and 4). The AUCs of $E_{\text{max}}$ and $E_{\text{mean}}$ were 0.769 (95% CI: 0.671, 0.868) and 0.730 (95% CI: 0.623, 0.838). The sensitivity, specificity, PPV and NPV of $E_{\text{max}}$ and $E_{\text{mean}}$ were 67.5%, 80%, 73.0%, 75.5% and 62.5%, 80%, 71.4%, 72.7%, respectively (Table 2).

*Diagnostic performance of STE parameters around lesions ($E_{max\text{-}shell}$, $E_{mean\text{-}shell}$)*

The elastographic values of different shell sizes ($E_{\text{max-shell-0.5}}$, $E_{\text{mean-shell-0.5}}$, $E_{\text{max-shell-1.0}}$, $E_{\text{mean-shell-1.0}}$, $E_{\text{max-shell-1.5}}$, $E_{\text{mean-shell-1.5}}$, $E_{\text{max-shell-2.0}}$, $E_{\text{mean-shell-2.0}}$) also differed significantly between benign and malignant

Table 2. Diagnostic performance of BI-RADS category and quantitative elastic values

| | Mean (kPa) | | Sensitivity (%) | Specificity (%) | PPV (%) | NPV (%) | AUC(95% CI) | Cutoffvalue | *p*Value |
|---|---|---|---|---|---|---|---|---|---|
| | Benign | Malignant | | | | | | | |
| BI-RADS | — | — | 95.0 | 32.0 | 70.4 | 94.4 | 0.635 (0.521, 0.749) | >3 | <0.001 |
| $E_{max}$ | 39.66 | 71.02 | 67.5 | 80.0 | 73.0 | 75.5 | 0.769 (0.671, 0.868) | >43.84 | <0.001 |
| $E_{mean}$ | 15.08 | 20.60 | 62.5 | 80.0 | 71.4 | 72.7 | 0.730 (0.623, 0.838) | >18.29 | <0.001 |
| $E_{max\text{-}shell\text{-}0.5}$ | 44.97 | 75.20 | 77.5 | 74.0 | 70.5 | 80.4 | 0.795 (0.702, 0.889) | >47.69 | <0.001 |
| $E_{mean\text{-}shell\text{-}0.5}$ | 15.74 | 23.78 | 75.0 | 76.0 | 71.4 | 79.2 | 0.785 (0.689, 0.881) | >14.91 | <0.001 |
| $E_{max\text{-}shell\text{-}1.0}$ | 44.37 | 90.53 | 80.0 | 84.0 | 80.0 | 84.0 | 0.852 (0.770, 0.933) | >60.03 | <0.001 |
| $E_{mean\text{-}shell\text{-}1.0}$ | 15.28 | 23.67 | 77.5 | 72.0 | 68.9 | 80.0 | 0.811 (0.722, 0.900) | >15.92 | <0.001 |
| $E_{max\text{-}shell\text{-}1.5}$ | 45.87 | 98.35 | 82.5 | 86.0 | 82.5 | 86.0 | 0.854 (0.765, 0.943) | >60.62 | <0.001 |
| $E_{mean\text{-}shell\text{-}1.5}$ | 17.05 | 25.01 | 65.0 | 82.0 | 74.3 | 74.5 | 0.775 (0.677, 0.874) | >24.56 | <0.001 |
| $E_{max\text{-}shell\text{-}2.0}$ | 44.84 | 119.79 | 87.5 | 88.0 | 85.4 | 89.8 | 0.930 (0.878, 0.983) | >67.55 | <0.001 |
| $E_{mean\text{-}shell\text{-}2.0}$ | 17.59 | 25.32 | 65.0 | 82.0 | 74.3 | 74.5 | 0.793 (0.701, 0.885) | >25.72 | <0.001 |
| $E_{max\text{-}shell\text{-}2.0}$ + age | — | — | 72.5 | 94.0 | 90.6 | 81.0 | 0.923 (0.872, 0.975) | | <0.001 |

AUC = the area under the receiver operating characteristic curve; BI-RADS = Breast Imaging Reporting and Data System; CI = confidence interval; NPV = negative predictive value; PPV = positive predictive value.

breast lesions ($p < 0.05$) (Figs. 3 and 4). Among these parameters, $E_{max\text{-}shell\text{-}2.0}$ yielded the highest AUC, 0.930 (95% CI: 0.878, 0.983), with a sensitivity, specificity, PPV and NPV of 87.5%, 88%, 85.4%, 89.8%. The AUC of $E_{max\text{-}shell\text{-}2.0}$ was higher than that of conventional ultrasound, which indicates that $E_{max\text{-}shell\text{-}2.0}$ has the highest diagnostic value in predicting malignant masses (Table 2).

*Multivariate logistic regression analysis*

Univariate analysis revealed that age, $E_{max}$, $E_{mean}$ and different $E_{max\text{-}shell}$ and $E_{mean\text{-}shell}$ values significantly differed for the identification of benign and malignant breast masses. These values were further analyzed using stepwise multivariate logistical regression. On logistical regression analysis, $E_{max\text{-}shell\text{-}2.0}$ and age were significantly independent predictors of malignancy with odds ratios (ORs) of 1.140 (95% CI: 1.038, 1.252, $p < 0.05$) and 1.161 (95% CI: 1.036, 1.300, $p < 0.05$), respectively (Table 3). The result of the LR test was significant (all $p < 0.05$), while the Hosmer−Lemeshow goodness-of-fit test was not ($p > 0.05$), suggesting that the overall model fit was good. Multivariate regression analysis revealed that $E_{max\text{-}shell\text{-}2.0}$ + age had an AUC of 0.923 (95% CI: 0.872, 0.975), with a sensitivity and specificity of 72.5% and 94%, respectively (Fig. 5). Combination of $E_{max\text{-}shell\text{-}2.0}$ with age improved the specificity and positive predictive value; however, the sensitivity, negative predictive value and AUC were reduced (Table 2).

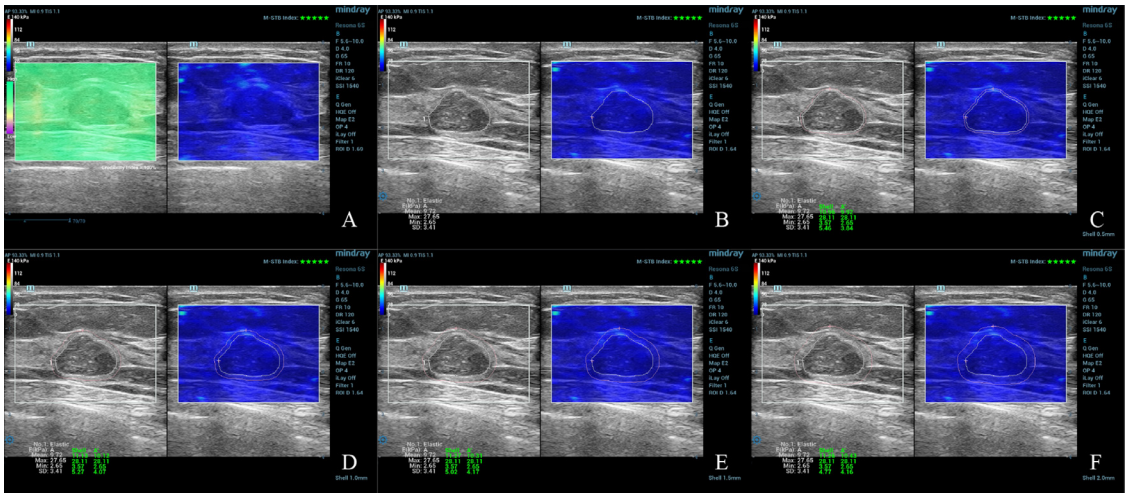


Fig. 3. Patient with fibroadenoma. (A) STE quality control with no obvious artifacts. (B) $E_{max}$ and $E_{mean}$ values of the lesion were 27.65 and 9.72kPa, respectively. (C) The shell measurement function included 0.5 mm of peripheral tissue around the breast lesion contour on the STE image. $E_{max\text{-}shell\text{-}0.5}$ and $E_{mean\text{-}shell\text{-}0.5}$ values were 28.11 and 10.96 kPa, respectively. (D) The shell included 1.0 mm of peripheral tissue. $E_{max\text{-}shell\text{-}1.0}$ and $E_{mean\text{-}shell\text{-}1.0}$ values were 28.11 and 11.13 kPa, respectively. (E) The shell included 1.5 mm of peripheral tissue. $E_{max\text{-}shell\text{-}1.5}$ and $E_{mean\text{-}shell\text{-}1.5}$ were 28.11 and 11.27 kPa, respectively. (F) The shell included 2.0 mm of peripheral tissue. $E_{max\text{-}shell\text{-}2.0}$ and $E_{mean\text{-}shell\text{-}2.0}$ values were 28.11 and 11.26 kPa, respectively. STE = sound touch shear wave elastography.

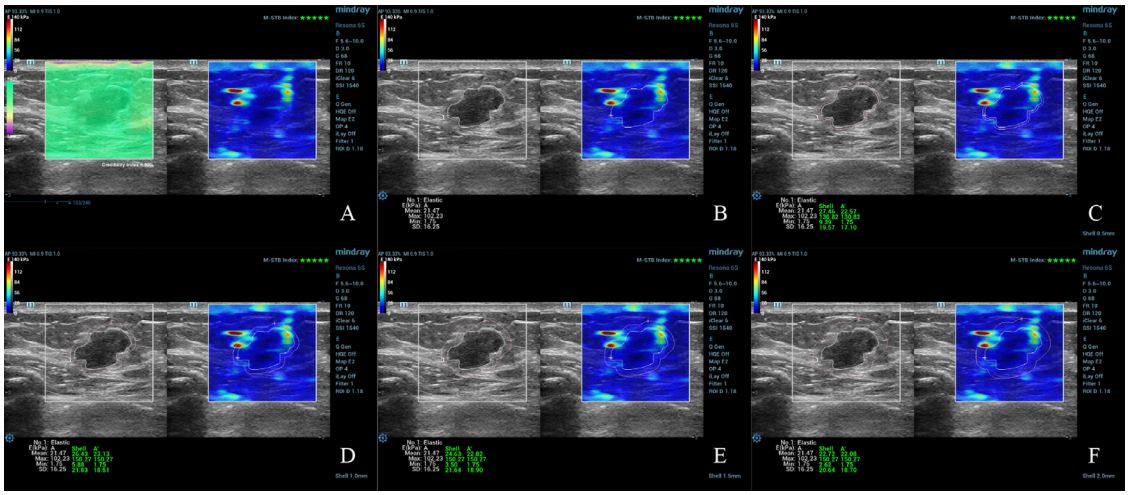


Fig. 4. Patient with invasive ductal carcinoma. (A) STE quality control with no obvious artifacts. (B) $E_{max}$ and $E_{mean}$ values of the mass were 102.23 and 21.47kPa, respectively. (C) The shell measurement function included 0.5 mm of peripheral tissue around the breast mass contour on the STE image. $E_{max\text{-}shell\text{-}0.5}$ and $E_{mean\text{-}shell\text{-}0.5}$ values were 130.82 and 27.46 kPa, respectively. (D) The shell included 1.0 mm of peripheral tissue. $E_{max\text{-}shell\text{-}1.0}$ and $E_{mean\text{-}shell\text{-}1.0}$ values were 150.27 and 26.43 kPa, respectively. (E) The shell included 1.5 mm of peripheral tissue. $E_{max\text{-}shell\text{-}1.5}$ and $E_{mean\text{-}shell\text{-}1.5}$ values were 150.27 and 24.63 kPa, respectively. (F) The shell included 2.0 mm of peripheral tissue. $E_{max\text{-}shell\text{-}2.0}$ and $E_{mean\text{-}shell\text{-}2.0}$ values were 150.27 and 22.72 kPa, respectively. STE = sound touch shear wave elastography.

### *Correlation between collagen fiber content and different* $E_{max\text{-}shell}$ *values*

Collagen fiber content of tissue around benign lesions (0.5, 1.0, 1.5 and 2.0 mm) was significantly lower than that of tissue around malignant lesions ($p < 0.05$) (Table 4). All $E_{max\text{-}shell}$ values positively correlated with collagen fiber content (Table 5). Collagen fiber content of surrounding tissue in the malignant group was highly correlated with the corresponding $E_{max\text{-}shell}$ values, among which $E_{max\text{-}shell\text{-}2.0}$ was the most highly correlated ($r = 0.853$, $p < 0.001$), whereas in the benign group, collagen fiber content was moderately correlated with all $E_{max\text{-}shell}$ values (Fig. 6).

## DISCUSSION

The BI-RADS classification of conventional ultrasound has been widely used to diagnose breast masses since it was first proposed. It has high sensitivity but relatively low specificity, especially in category 4a with a probability of malignancy 2%−10%, which often results in unnecessary biopsy and excessive diagnosis (Yoon et al. 2013). The BI-RADS category of a breast lesion is determined by the characteristics revealed by 2-D gray-scale ultrasonography (Choi et al. 2019). However, malignant and benign breast masses often overlap to some extent in 2-D gray-scale ultrasonography, which

Table 3. Logistical regression analysis to identify factors that predicted breast malignancy

| Variable | Univariate analysis | | | Multivariate analysis | | |
|---|---|---|---|---|---|---|
| | $\beta$ | OR (95% CI) | p Value | $\beta$ | OR (95% CI) | p Value |
| $E_{max}$ | 0.042 | 1.043 (1.019−1.068) | <0.001 | −0.003 | 0.997 (0.950−1.046) | 0.902 |
| $E_{mean}$ | 0.148 | 1.159 (1.070−1.256) | <0.001 | −0.005 | 0.995 (0.809−1.224) | 0.963 |
| *E*max-shell-0.5 | 0.044 | 1.045 (1.023−1.067) | <0.001 | 0.016 | 1.016 (0.969−1.066) | 0.515 |
| *E*mean-shell-0.5 | 0.093 | 1.098 (1.042−1.156) | <0.001 | 0.003 | 1.003 (0.881−1.143) | 0.962 |
| *E*max-shell-1.0 | 0.054 | 1.055 (1.031−1.080) | <0.001 | −0.002 | 0.998 (0.929−1.072) | 0.947 |
| *E*mean-shell-1.0 | 0.140 | 1.150 (1.076−1.230) | <0.001 | −0.019 | 0.981 (0.826−1.165) | 0.829 |
| *E*max-shell-1.5 | 0.058 | 1.059 (1.034−1.086) | <0.001 | −0.083 | 0.921 (0.843−1.005) | 0.066 |
| *E*mean-shell-1.5 | 0.140 | 1.150 (1.077−1.228) | <0.001 | −0.066 | 0.936 (0.749−1.169) | 0.558 |
| *E*max-shell-2.0 | 0.055 | 1.056 (1.035−1.078) | <0.001 | 0.131 | 1.140 (1.038−1.252) | 0.006* |
| *E*mean-shell-2.0 | 0.113 | 1.119 (1.055−1.187) | <0.001 | 0.119 | 1.127 (0.957−1.326) | 0.152 |
| Age | 0.114 | 1.120 (1.063−1.180) | <0.001 | 0.149 | 1.161 (1.036−1.300) | 0.010* |

CI = confidence interval; OR = odds ratio.
* Statistically significant difference ($p < 0.05$).

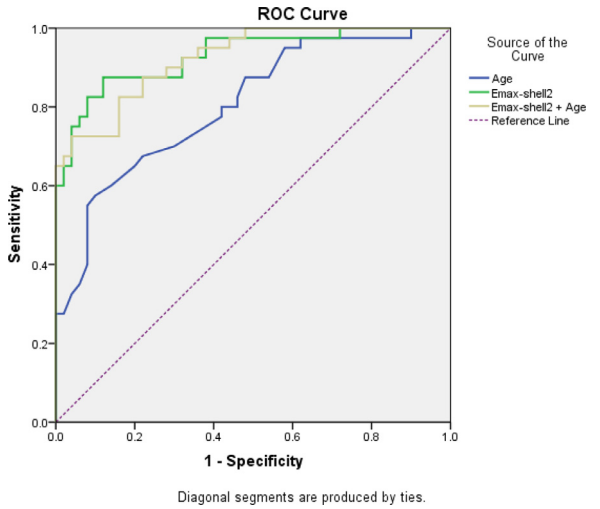


Fig. 5. Receiver operating characteristic (ROC) curves of $E_{max\text{-}shell\text{-}2.0}$, age and $E_{max\text{-}shell\text{-}2.0}$ + age values for analyzing diagnostic performance.

makes their differentiation difficult (Barr 2019). With the development of elastography technology, we can observe not only the morphology and internal blood flow characteristics of the lesion, but also the stiffness in and around the masses, which improves accuracy in diagnosing breast malignancy (Łukasiewicz et al. 2017).

Previous studies have reported that the peripheral tissue of malignant lesions is typically stiffer than that of benign lesions because the former have abnormal stiff collagen fiber, which is related to cancer fibroblasts, as well as infiltration of cancer cells into the surrounding tissue (Xiao et al. 2017). Other studies have revealed that peritumoral invasion is an independent prognostic factor significantly associated with increased risk of relapse and death in node-negative breast cancer patients (Colleoni et al. 2007; Tozaki and Fukuma 2011; Wernicke et al. 2011; Evans et al. 2012). On this basis, investigating the stiffness of tissues around breast masses seems to be of great significance. Evans et al. (2010) and Tozaki and Fukuma (2011) reported that the stiffest part of malignant breast masses is in the periphery of the mass, rather than in the interior, and is defined as the "stiff rim" sign on the color elastography map. Two reasons can be ascribed to this phenomenon. One is the

Table 4. Collagen fiber content of breast lesions of different shell size

| Shell size | Collagen fiber content (%) | | *p* Value |
|---|---|---|---|
| | Benign (n = 50) | Malignant (n = 40) | |
| 0.5 mm | 11.81 ± 4.75 | 21.84 ± 7.96 | <0.001 |
| 1.0 mm | 11.43 ± 2.27 | 22.98 ± 7.70 | <0.001 |
| 1.5 mm | 11.97 ± 2.41 | 27.63 ± 7.70 | <0.001 |
| 2.0 mm | 11.29 ± 2.76 | 30.80 ± 6.34 | <0.001 |

Table 5. Correlation between all $E_{max\text{-}shell}$ values and collagen fiber content

| | Collagen fiber content | |
|---|---|---|
| | Spearman's *r* | *p* Value |
| Benign | | |
| $E_{max\text{-}shell\text{-}0.5}$ | 0.606 | <0.001 |
| $E_{max\text{-}shell\text{-}1.0}$ | 0.653 | <0.001 |
| $E_{max\text{-}shell\text{-}1.5}$ | 0.662 | <0.001 |
| $E_{max\text{-}shell\text{-}2.0}$ | 0.681 | <0.001 |
| Malignant | | |
| $E_{max\text{-}shell\text{-}0.5}$ | 0.822 | <0.001 |
| $E_{max\text{-}shell\text{-}1.0}$ | 0.831 | <0.001 |
| $E_{max\text{-}shell\text{-}1.5}$ | 0.847 | <0.001 |
| $E_{max\text{-}shell\text{-}2.0}$ | 0.853 | <0.001 |

desmoplastic reaction or infiltration of cancer cells into the stroma, which induces the hardness of peripheral tissue. The other is the attenuation of the energy of shear waves in surrounding regions, which leads to lower elastic values inside breast lesions (Evans et al. 2010; Yang et al. 2020). Zhou et al. (2014a, 2014b) proposed that the "stiff rim" sign is able to differentiate breast masses. However, it is a qualitative evaluation that is influenced by the elasticity range setting of the color-coded elastographic image. In this study, we applied the STE shell toolbox to describe elastic characteristics of tissues in different regions (0.5, 1, 1.5 and 2.0 mm) around the mass quantitatively. In contrast to other elastic methods in which the operator selects the hardest or softest part to measure the value of elasticity, STE automatically measures the value of elasticity by taking tissue samples from the entire annular area in or around the mass and is therefore less affected by the operator (Huang et al. 2019).

In our study, $E_{max}$ and $E_{mean}$ were significantly higher in malignant lesions than benign lesions ($p < 0.05$), which is consistent with previous literature (Shiina et al. 2015; Song et al. 2018). $E_{max\text{-}shell}$ and $E_{mean\text{-}shell}$ values were also higher in malignant than in benign masses ($p < 0.05$). Moreover, the results revealed that maximum elastic values either inside or around breast masses were all better than mean values with respect to diagnostic performance. We hypothesized that this may be due to the highly active proliferation and remodeling of the extracellular matrix in tumors with collagen fibers as the main component, which significantly increases tissue stiffness, whereas in benign lesions this would not occur. However, tumor active proliferation can also lead to local ischemia, necrosis, cystic changes, and so on, affecting the average hardness of tissues. Therefore, the maximum elasticity may play a better role in predicting potential malignancy. Among these maximum elastic parameters, $E_{max\text{-}shell\text{-}2.0}$ yielded the highest AUC of 0.930, with a sensitivity of 87.5% and a

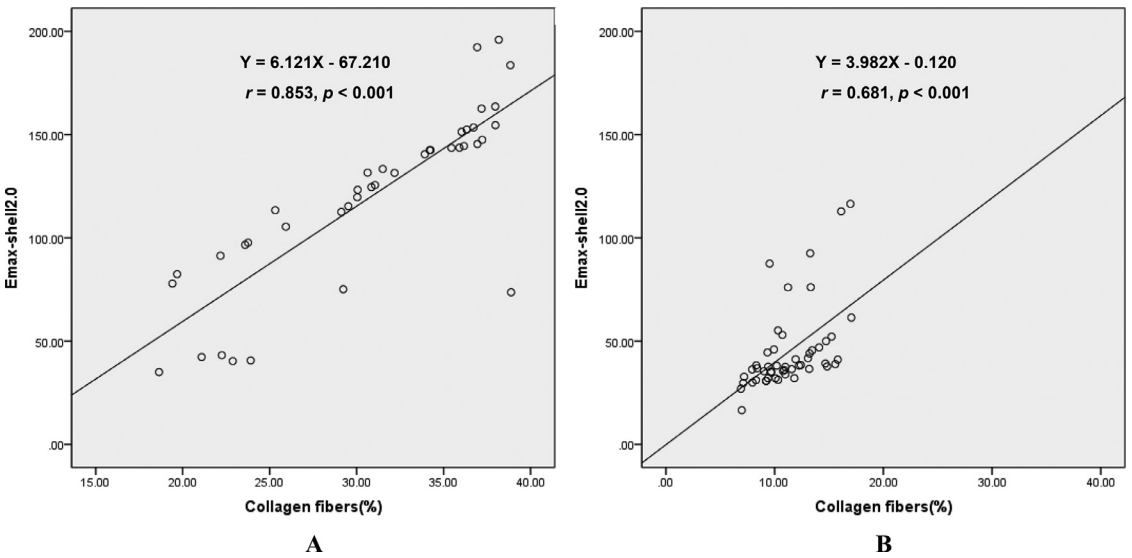


Fig. 6. (A) Strong positive correlations between collagen fiber content of 2-mm tissues around breast masses and $E_{max\text{-}shell\text{-}2.0}$ in the malignant group ($r = 0.853$, $p < 0.001$). (B) Moderate positive correlations in the benign group ($r = 0.681$, $p < 0.001$).

specificity of 88%, in distinguishing malignant breast masses. Moreover, $E_{max\text{-}shell\text{-}2.0}$ correlated best with collagen fiber content in this study, indicating that $E_{max\text{-}shell\text{-}2.0}$ performed best in reflecting collagen fiber content. Collectively, $E_{max\text{-}shell\text{-}2.0}$ had the highest diagnostic value for malignant lesions, which was consistent with previous published literature (Park et al. 2018).

We observed a high positive correlation between collagen fiber content and the corresponding $E_{max\text{-}shell}$ values of the malignant group, especially $E_{max\text{-}shell\text{-}2.0}$. Moreover, the quantity of collagen fibers in the tissues around malignant masses was significantly higher than that of tissues around benign masses according to the histopathological results. Therefore, we speculate that the $E_{max\text{-}shell}$ of STE is valuable in diagnosing malignant breast masses by reflecting the collagen fiber content, which deserves investigation in depth in the future.

In the present study, patients with malignant lesions were statistically older than those with benign lesions. Age is always recognized as an important clinical factor by both clinicians and ultrasound physicians (Verdial et al. 2017). Multivariate logistic regression analysis indicates that $E_{max\text{-}shell\text{-}2.0}$ and age were found to be significant independent predictors of malignancy. Conventional ultrasound examination combined with STE can provide a more comprehensive understanding of the tumor, thus better guiding follow-up treatment strategies.

There are some limitations to this study. First, it is a single-center study based at one hospital and the sample size was limited; therefore, there were not enough pathological types of lesions, and we were unable to perform classification analysis of different pathological types of breast lesions. Second, it is not clear whether breast density and mass depth can influence elasticity characteristics. Third, BI-RADS 3 patients, for whom short-term follow-up imaging is recommended rather than surgery, were included in this study, which may lead to selection bias. Collectively, further multicenter research studies with larger populations are required to provide more comprehensive and stronger evidence.

## CONCLUSIONS

This study indicates that tissue stiffness around breast lesions measured by STE is a useful metric in identifying malignant breast masses as it reflects collagen fiber content, and the maximum Young's modulus of tissues in the 2-mm annular region surrounding the mass performs best among all the elasticity measurements.

*Conflict of interest disclosure*—The authors have no conflicts of interest or sources of funding to declare.

## REFERENCES

Altıntas Y, Bayrak M, Alabaz Ö, Celiktas M. A qualitative and quantitative assessment of simultaneous strain, shear wave, and point shear wave elastography to distinguish malignant and benign breast lesions. Acta Radiol 2021;62:1155–1162.

Balleyguier C, Ciolovan L, Ammari S, Canale S, Sethom S, Al Rouhbane R, Vielh P, Dromain C. Breast elastography: The technical process and its applications. Diagn Interv Imaging 2013;94:503–513.

Barr RG. Future of breast elastography. Ultrasonography 2019;38:93–105.

Barr RG, Nakashima K, Amy D, Cosgrove D, Farrokh A, Schafer F, Bamber JC, Castera L, Choi BI, Chou YH, Dietrich CF, Ding H, Ferraioli G, Filice C, Friedrich-Rust M, Hall TJ, Nightingale KR, Palmeri ML, Shiina T, Suzuki S, Sporea I, Wilson S, Kudo M. WFUMB guidelines and recommendations for clinical use of ultrasound elastography: Part 2: breast. Ultrasound Med Biol 2015;41:1148–1160.

Berg WA, Bandos AI, Mendelson EB, Lehrer D, Jong RA, Pisano ED. Ultrasound as the primary screening test for breast cancer: Analysis From ACRIN 6666. J Natl Cancer Inst 2015;108:djv367.

Choi HY, Seo M, Sohn YM, Hwang JH, Song EJ, Min SY, Kang HJ, Han DY. Shear wave elastography for the diagnosis of small (≤2 cm) breast lesions: Added value and factors associated with false results. Br J Radiol 2019;92 20180341.

Colleoni M, Rotmensz N, Maisonneuve P, Sonzogni A, Pruneri G, Casadio C, Luini A, Veronesi P, Intra M, Galimberti V, Torrisi R, Andrighetto S, Ghisini R, Goldhirsch A, Viale G. Prognostic role of the extent of peritumoral vascular invasion in operable breast cancer. Ann Oncol 2007;18:1632–1640.

Dong F, Wu H, Zhang L, Tian H, Liang W, Ye X, Liu Y, Xu J. Diagnostic performance of multimodal sound touch elastography for differentiating benign and malignant breast masses. J Ultrasound Med 2019;38:2181–2190.

Evans A, Whelehan P, Thomson K, McLean D, Brauer K, Purdie C, Jordan L, Baker L, Thompson A. Quantitative shear wave ultrasound elastography: initial experience in solid breast masses. Breast Cancer Res 2010;12:R104.

Evans A, Whelehan P, Thomson K, McLean D, Brauer K, Purdie C, Baker L, Jordan L, Rauchhaus P, Thompson A. Invasive breast cancer: Relationship between shear-wave elastographic findings and histologic prognostic factors. Radiology 2012;263:673–677.

Farooq F, Mubarak S, Shaukat S, Khan N, Jafar K, Mahmood T, Saeed MA. Value of elastography in differentiating benign from malignant breast lesions keeping histopathology as gold standard. Cureus 2019;11:e5861.

Geisel J, Raghu M, Hooley R. The role of ultrasound in breast cancer screening: The case for and against ultrasound. Semin Ultrasound CT MR 2018;39:25–34.

Huang L, Ma M, Du Z, Liu Z, Gong X. Quantitative evaluation of tissue stiffness around lesion by sound touch elastography in the diagnosis of benign and malignant breast lesions. PLoS One 2019;14 e0219943.

Lin X, Chang C, Wu C, Chen Q, Peng Y, Luo B, Tang L, Li J, Zheng J, Zhou R, Cui G, Li A, Wang X, Qian L, Zhang J, Wen C, Gay J, Zhang H, Li A, Chen Y. Confirmed value of shear wave elastography for ultrasound characterization of breast masses using a conservative approach in Chinese women: A large-size prospective multicenter trial. Cancer Manag Res 2018;10:4447–4458.

Łukasiewicz E, Ziemiecka A, Jakubowski W, Vojinovic J, Bogucevska M, Dobruch-Sobczak K. Fine-needle versus core-needle biopsy—Which one to choose in preoperative assessment of focal lesions in the breasts? Literature review. J Ultrason 2017;17:267–274.

Mesurolle B, El Khoury M, Chammings F, Zhang M, Sun S. Breast sonoelastography: Now and in the future. Diagn Interv Imaging 2019;100:567–577.

Mitchell EP. U.S. Preventive Services Task Force Final Recommendation Statement: Evidence summary, and modeling studies on screening for lung cancer. J Natl Med Assoc 2021;113:239–240.

Mukaka MM. Statistics corner: A guide to appropriate use of correlation coefficient in medical research. Malawi Med J 2012;24:69–71.

Ophir J, Céspedes I, Ponnekanti H, Yazdi Y, Li X. Elastography: A quantitative method for imaging the elasticity of biological tissues. Ultrason Imaging 1991;13:111–134.

Park HS, Shin HJ, Shin KC, Cha JH, Chae EY, Choi WJ, Kim HH. Comparison of peritumoral stromal tissue stiffness obtained by shear wave elastography between benign and malignant breast lesions. Acta Radiol 2018;59:1168–1175.

Peairs KS, Choi Y, Stewart RW, Sateia HF. Screening for breast cancer. Semin Oncol 2017;44:60–72.

Ricci P, Maggini E, Mancuso E, Maldur V, Medvedyeva O, Ursu SC, Pediconi F. Elastography in the diagnosis of breast lesions: Comparison of different elastographic features. Acta Radiol 2017;58:1189–1197.

Rossi L, Mazzara C, Pagani O. Diagnosis and treatment of breast cancer in young women. Curr Treat Options Oncol 2019;20:86.

Shi XQ, Li J, Qian L, Xue X, Li J, Wan W. Correlation between elastic parameters and collagen fibre features in breast lesions. Clin Radiol 2018;73:595. e1−595.e7.

Shiina T, Nightingale KR, Palmeri ML, Hall TJ, Bamber JC, Barr RG, Castera L, Choi BI, Chou YH, Cosgrove D, Dietrich CF, Ding H, Amy D, Farrokh A, Ferraioli G, Filice C, Friedrich-Rust M, Nakashima K, Schafer F, Sporea I, Suzuki S, Wilson S, Kudo M. WFUMB guidelines and recommendations for clinical use of ultrasound elastography: Part 1. Basic principles and terminology. Ultrasound Med Biol 2015;41:1126–1147.

Song EJ, Sohn YM, Seo M. Diagnostic performances of shear-wave elastography and B-mode ultrasound to differentiate benign and malignant breast lesions: The emphasis on the cutoff value of qualitative and quantitative parameters. Clin Imaging 2018;50:302–307.

Tozaki M, Fukuma E. Pattern classification of ShearWave$^{TM}$ Elastography images for differential diagnosis between benign and malignant solid breast masses. Acta Radiol 2011;52:1069–1075.

Verdial FC, Etzioni R, Duggan C, Anderson BO. Demographic changes in breast cancer incidence, stage at diagnosis and age associated with population-based mammographic screening. J Surg Oncol 2017;115:517–522.

Wernicke M, Roitman P, Manfre D, Stern R. Breast cancer and the stromal factor: The "prometastatic healing process" hypothesis. Medicina (B Aires) 2011;71:15–21.

Winters S, Martin C, Murphy D, Shokar NK. Breast cancer epidemiology, prevention, and screening. Prog Mol Biol Transl Sci 2017;151:1–32.

Xia S, Ren X, Ni Z, Zhan W. A Noninvasive method-shear-wave elastography compared with transient elastography in evaluation of liver fibrosis in patients with chronic hepatitis B. Ultrasound Q 2019;35:147–152.

Xiao Y, Yu Y, Niu L, Qian M, Deng Z, Qiu W, Zheng H. Quantitative evaluation of peripheral tissue elasticity for ultrasound-detected breast lesions. Clin Radiol 2016;71:896–904.

Xiao Y, Zeng J, Zhang X, Niu LL, Qian M, Wang CZ, Zheng HR, Zheng RQ. Ultrasound strain elastography for breast lesions: Computer-aided evaluation with quantifiable elastographic features. J Ultrasound Med 2017;36:1089–1100.

Yang H, Xu Y, Zhao Y, Yin J, Chen Z, Huang P. The role of tissue elasticity in the differential diagnosis of benign and malignant breast lesions using shear wave elastography. BMC Cancer 2020;20:930.

Yoon JH, Jung HK, Lee JT, Ko KH. Shear-wave elastography in the diagnosis of solid breast masses: what leads to false-negative or false-positive results?. Eur Radiol 2013;23:2432–2440.

Zhang L, Ding Z, Dong F, Wu H, Liang W, Tian H, Ye X, Luo H, Xu J. Diagnostic performance of multiple sound touch elastography for differentiating benign and malignant thyroid nodules. Front Pharmacol 2018;9:1359.

Zhang L, Xu J, Wu H, Liang W, Ye X, Tian H, Dong F. Screening breast lesions using shear modulus and its 1-mm shell in sound touch elastography. Ultrasound Med Biol 2019;45:710–719.

Zhou J, Zhan W, Chang C, Zhang X, Jia Y, Dong Y, Zhou C, Sun J, Grant EG. Breast lesions: Evaluation with shear wave elastography, with special emphasis on the "stiff rim" sign. Radiology 2014a;272:63–72.

Zhou J, Zhan W, Dong Y, Yang Z, Zhou C. Stiffness of the surrounding tissue of breast lesions evaluated by ultrasound elastography. Eur Radiol 2014b;24:1659–1667.